Agreement INGV-DPC 2007-2009

Project S1: Analysis of the seismic potential in Italy for the evaluation of the seismic hazard

Responsibles: Salvatore Barba, Istituto Nazionale di Geofisica e Vulcanologia, and Carlo Doglioni, Università di Roma "La Sapienza"

http://groups.google.com/group/INGV-DPC-2007-S1
(restricted access)

Deliverable # 3.01.1
Technical report illustrating the results obtained in the Crotone Peninsula based on geological and InSAR data

May 31st, 2010

prepared by:
UR3.01, Resp. Roberto Basili, INGV, Sezione di Sismologia e Tettonofisica

UR3.01, Salvatore Barba, Pierfrancesco Burrato, Umberto Fracassi, Vanja Kastelic, Mara Monica Tiberti, Paola Vannoli, INGV, Sezione di Sismologia e Tettonofisica
UR3.01, Salvatore Stramondo, Cristiano Tolomei, INGV, Centro Nazionale Terremoti
Michele Soligo, Paola Tuccimei, Università di Roma Tre

1. Description of the Deliverable

This work was aimed at collecting data to estimating the rate of uplift over several temporal scales. The analysis includes a very short-term analysis (tens of years) of InSAR data, a middle-term analysis of Holocene geological data, and a long-term analysis of Middle-Late Pleistocene geological data. After a preliminary reconnaissance in a large area, all final datasets focus strictly on the area of the Crotone Peninsula. The techniques applied span from Small Baseline Subset Interferometric SAR, to classic geomorphic and stratigraphic analysis aided by radiocarbon and U/Th dating.

Geomorphic Analysis methods

The geomorphic analysis of both Holocene and Pleistocene features was based on two sets of aerial photographs (GAI 1955 survey, at nominal scale of 1.33,000, and Volo Italia 1994 survey, at nominal scale of 1:70,000), topographic maps at a scale of 1:10,000 and Digital Elevation Model at 40 m cell spacing from Regione Calabria, Handheld GPS Garmin GPSmap 60CSx, and Wild TC1610 Total Station Leica Heerbrugg Theodolite.

Late Pleistocene terrace morphology

Three major treads were identified by mapping all terrace remnants lager than 0.1 km^2 (Figure 1, Table 1). The entire step-like sequence of terrace treads is well exposed in the southern part of the area in the Le Castella and Capo Rizzuto promontories. Here the inner edge of the lower terrace runs at an elevation of about 40-50 meters and the riser between the lower and middle terrace treads marks the transition between a clastic depositional body and a biogenic body. The inner edge of the middle tread runs at about 60-70 meters and the riser between the middle and upper terrace treads exposes the underlying older marine clay. The middle tread is the largest and can be followed for several kilometers. The inner edge of the upper tread reaches at places 90-100 meters. In the northeast sector of the area, capo Cimiti and Capo Colonna, the lower tread was not found or, more simply, the facies transition is smoother and not marked in the morphology. Here the elevation of remnants is generally lower than elsewhere. In addition, several landslides affect the original morphology of the terrace.

Late Pleistocene terrace stratigraphy

The three terrace levels illustrated above were surveyed in the entire area. The depositional body of the terrace is widely exposed, especially on the sea-facing steep cliff. The thickness of the terrace deposit is highly variable for it fills older deep incisions carved into the underlying Pliocene – Lower Pleistocene marine clay unit.

From top to bottom, the typical terrace depositional sequence is formed by (thickness values are given as an example from an exposure at Capo Colonna):

- Horizontally bedded, highly cemented, biogenic coarse calcarenite (1.20 m), rich in corals and marine shells. At places an Ostrea *sp*.-rich layer marks the base.
- Horizontally bedded, bioturbated coarse calcarenite (0.80 m).
- Horizontally bedded, parallel- and cross-laminated coarse-to-fine calcarenite (6.50 m).
- Marine-shell and coral-fragment rich, parallel-laminated, slightly cemented coarse calcarenite (0.80 m).
- Horizontally bedded, parallel- and cross-laminated coarse-to-fine calcarenite (2-4 m) laterally adjoining algal-concretion coated calcarenite boulders (2-5 m).
- Plio-Pleistocene massive to laminated grey clay.

Samples for U/Th dating were systematically collected from the upper layers (Table 1).

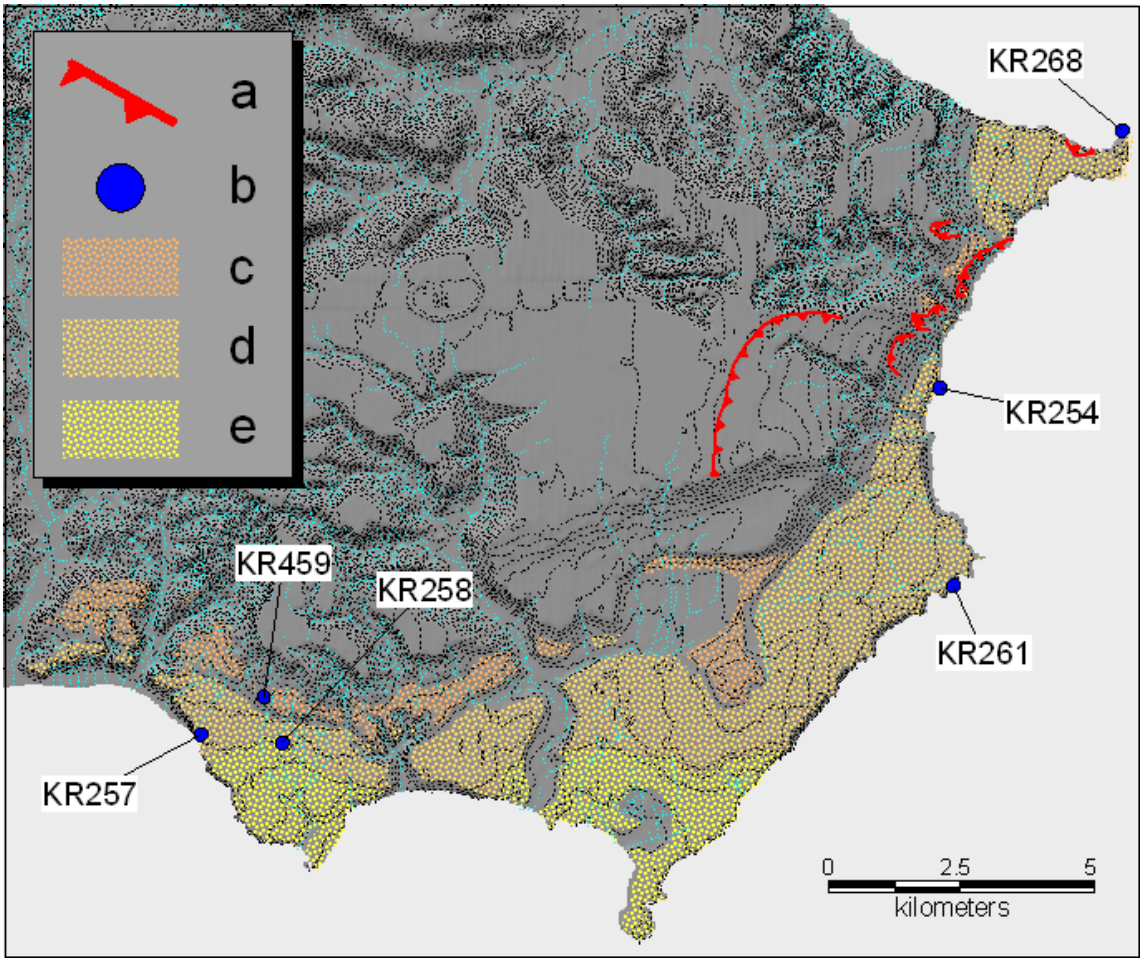

Figure 1 – Map of the Late Pleistocene terrace in the Crotone Peninsula. Legend: a) landslide scarp; b) U/Th dated sample location; c) upper terrace tread; d) middle terrace tread; e) lower terrace tread. Contour lines 10 m spaced.

Holocene raised shoreline

The detailed field survey was carried out for a 50-km long stretch of the coast in the Crotone Peninsula and led to the identification and classification of a number of sites with markers of possible Holocene emergence (Figure 2 and Table 2). All the sites are located along stretches of the coastline characterized by the presence of steep cliffs or rocky promontories.

The coastal morphology, outlined in Figure 2, is controlled by the Cutro unit, lightly consolidated marine clays (Pliocene – Early Pleistocene), and is generally characterized by tall steep cliffs carved into the clay and topped by coastal terraces, with narrow beaches in front of them. There are two notable exceptions to this general rule at Le Castella and Capo Colonna small peninsulas (sites n. 102 and 130-131, respectively), where the cliffs are carved directly into older units of the coastal terrace deposits. Outside the Crotone Peninsula the coast line is low with wide sandy beaches, and the raisers of the lowermost marine terraces are located few hundred of meters inland.

During our preliminary geomorphic analysis and the field survey we identified a total of 12 sites with clues of uplifted sea level proxies of possible Holocene age, or we suspected the preservation of these features to be possible. Only 2 sites returned to be devoid of any useful geomorphic feature, either because it was destroyed by the coastal evolution or by human activity (sites n. 112-113 and 133). Descriptions of all sites and relative markers are

summarized in Table 1. We used radiocarbon dating to discriminate between true Holocene features and older features.
The most common paleo sea level indicators were tidal notches, abrasion platforms and boulders encrusted with algal rims and/or lithophaga borings. We measured the elevation above sea level of all the markers with a spirit level and a graduated rod. We made corrections for the tide using the data of the nearest tide gauge that is located in the Crotone harbor.
In some sites we found contrasting evidences of possible Holocene uplift coming from boulders with shell borings located at the base of the cliff (e.g. site n. 101). At first glance they seemed to be exposures of the local bedrock, hence good indicators of uplift. A more detailed survey helped us realize they were fallen from the cliff and incorporated within the deposits of the coastal terrace. We also realized that at the base of each terrace body there is a boulder lag with shell borings and algal encrustation very similar to what looks like present day rocky shorelines. Therefore, all these sites were excluded from this analysis.
We identified two sites with the most reliable evidence of Holocene uplift: one already known in the literature, where we present new age determinations (Chiacolilli, site n. 126), and a new site where the evidence of uplift is supported by new age determinations and measurements of paleosealevel (Bosco Soverito, sites n. 103-111, 132).
Age and elevation of markers at both sites suggest an uplift value of at least 1 m in the last 2-3 ky. We also identified other indicators of emergence (tidal notches and abrasion platforms south of the Chiacolilli site) that could not be dated because of lack of datable samples. However, based on their elevation they correlate well with those that have been positively dated.

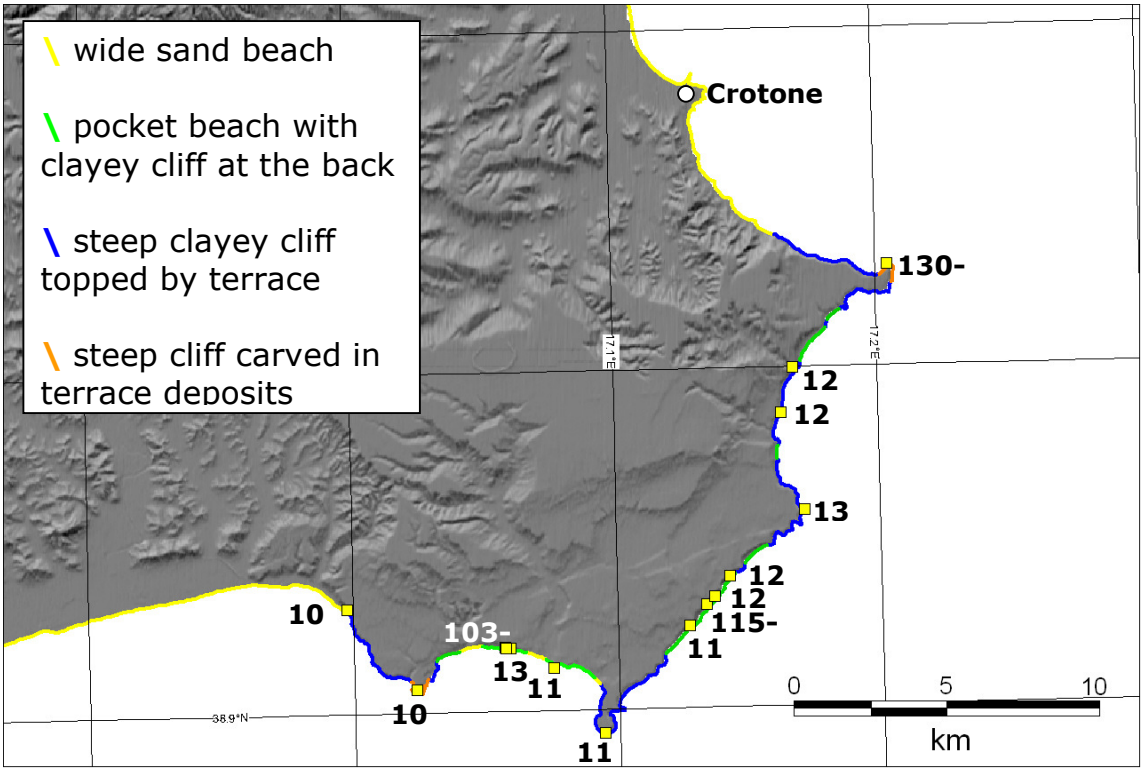

Figure 2 - Map of collected evidence of Holocene raised beaches (yellow squares). Numbers refer to the survey sites listed in Table 1.

U/Th Dating Analytical methods

Coral samples were preventively analyzed by XRD in order to indentify any trace of calcite recrystallization that would make unreliable chronological data.

Unaltered corals and other carbonate samples were spiked with a mixed ^{236}U-^{229}Th tracer and dissolved in concentrated distilled HCl. The dried chloride was then converted to nitrate. U and Th were separated on miniaturized PTFE columns containing U-TEVA™ resin using HNO_3 and HCl. As the Th eluate is strongly bound to rather volatile organic matter washed from the resin, the Th fraction was evaporated at < 50°C to avoid loss by evaporation. Organic molecules from the resin were observed in the past to cause three adverse effects: they increase proneness to obstruction of the sample uptake capillary, they coat the capillary, causing persistent memory effects, and they accumulate in the mass spectrometer flight tube, contributing an optical background radiation which simulates a high grey current in the ion counters, even at pressures of 10^{-7} Pa.

The oxidation protocol described by Hippler et al. (2004) only partially solves this problem. We found it necessary to resort to cold-plasma oxidation before analysis, using a Bio-Rad® PT 7100 RF plasma barrel etcher at 0.1 mbar oxygen pressure. Care must be taken not to exceed an output power of ca. 40 W, as otherwise the organic complexes bound to Th evaporate and the Th yield drops dramatically.

After oxidation, U and Th samples were dissolved in 3 M HCl, and measured on a Nu Instruments™ multicollector plasma source mass spectrometer equipped with an APEX™ desolvating nebulizer. The WARP™ filter limiting access to one of the ion counters of the mass spectrometer is able to reduce the background on masses 230 and 229 to less than 0.5 ppm and less than 0.2 ppm of the peak height at mass 232, respectively. Measurement protocols are as described by Fleitmann et al. (2007).

Ages are calculated using two different procedures: 3D-isochron (3DI) and single-point (SP) age. If the sample is affected by a negligible detrital fraction, indicated by a $^{230}Th/^{232}Th$ activity ratio higher than 20, a single-point approach is used to calculate the age. In case of a significant contamination, 3D-isochron is used. 3DI use 4 coeval subsamples. In order to calculate the ($^{230}Th/^{238}U$) and ($^{234}U/^{238}U$) activity ratios of the pure carbonate fraction, the four subsamples are plotted on a three-dimensional isochron, whereby the X, Y and Z axes are the ($^{232}Th/^{238}U$), ($^{230}Th/^{238}U$), and ($^{234}U/^{238}U$) activity ratios, respectively. Figure 3 shows a two dimensional projection, in which the intercept with the ($^{230}Th/^{238}U$) axis gives the detrital-corrected ($^{230}Th/^{238}U$) activity ratio. The ages of all samples were calculated by means of Isoplot/Ex (version 3.0), a plotting and regression program designed by Ludwig (2003) for radiogenic-isotope data. U-series data are reported in Table 3. Errors are quoted as 2 σ.

U/Th Dating Results

U content, U and Th activity ratios and age results of samples are reported in Table 3.

In Table 3, 3DI and SP data are reported. 3DI is the most rigorous approach, but associated ages are affected by larger errors. SP use the fresher available subsample and is affected by smaller errors. KR254 and KR268 samples are re-crystallized and ages are unreliable; KR257 and KR258 samples provide reliable results; KR 261 is slightly altered and chronological data need to be used with caution. KR257 3DI age = 138 ± 25 ka; SP age = 133 ± 3 ka; KR258 3DI age = 162 ± 68 ka; SP age = 119 ± 2 ka; KR261 3DI age = 118 ± 54 ka; SP age = 152 ± 4 ka. KR 459 A and KR 355 samples are not affected by contamination as shown by high $^{230}Th/^{232}Th$ activity ratio. Corresponding ages are: KR 459 A = 145 ± 4 ka, KR 355 = 7.6 ± 0.2 ka.

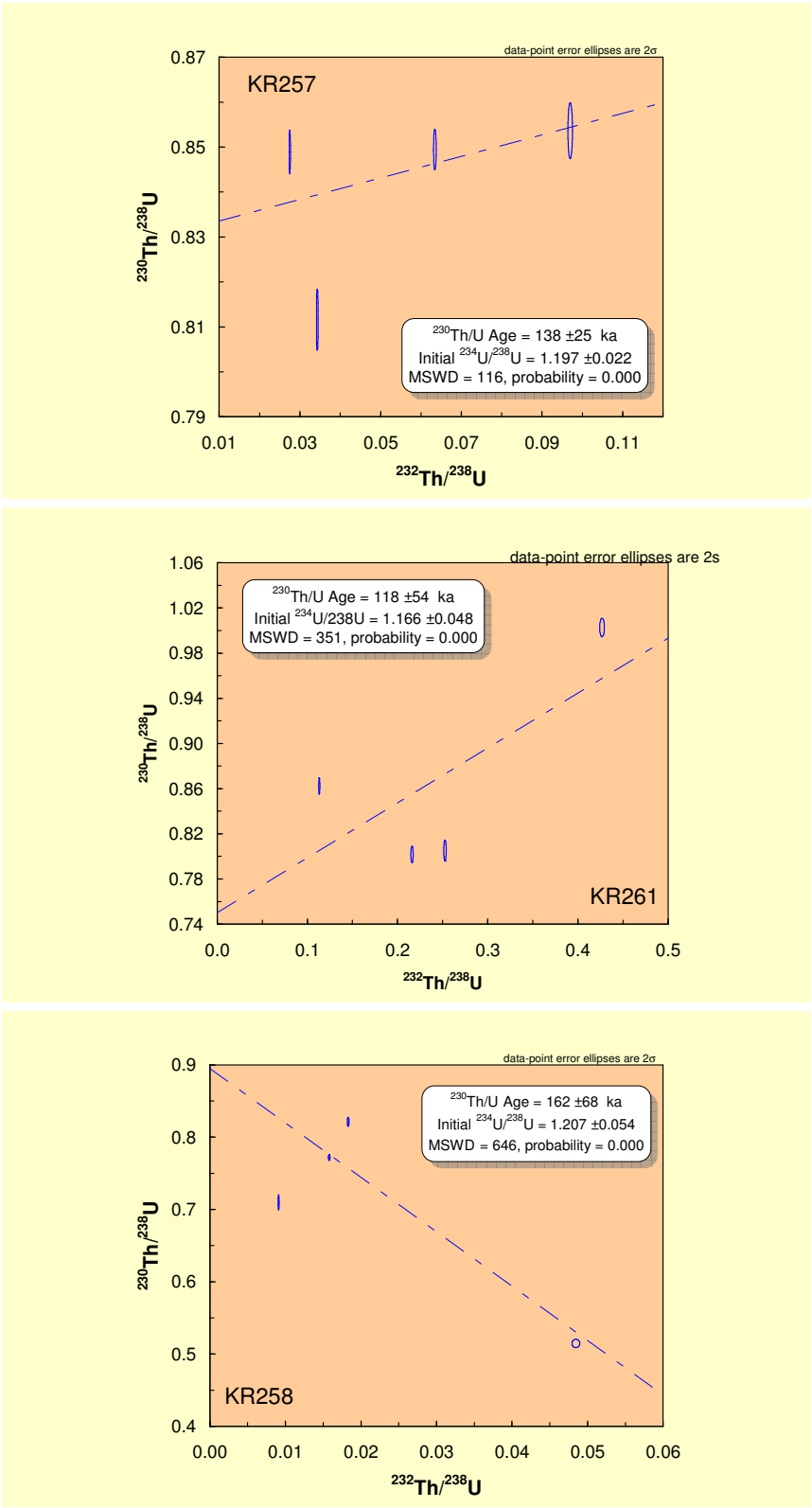

Figure 3 – Diagrams showing the two dimensional projection of 3DI plots (intercept with the ($^{230}Th/^{238}U$) axis gives the detrital-corrected ($^{230}Th/^{238}U$) activity ratio) for significantly contaminated samples.

Radiocarbon Dating Method

We adopted the AMS technique with calibration when possible. Samples deemed to be possibly of Holocene ages were sent to two different laboratories: Beta Analytic (http://www.radiocarbon.com/) and Poznan Radiocarbon Laboratory (http://www.radiocarbon.pl/). The results of radiocarbon dating are illustrated in Table 4.

Geological dataset

Information on the whole dataset is made available in a separate file with location of all the mapped sites of interests with associated ages, elevation measurements, paleosealevel elevation and descriptions. The table structure is illustrated below.

Data field	Definition
ID	*Identification number of the site*
Lat	*Latitude in decimal degrees (WGS84)*
Lon	*Longitude in decimal degrees (WGS84)*
SLP_Elev_m	*Elevation in meters of the geological remnant identified as being a paleo sea level proxy*
SLP_ElevErr_m	*Error in meters of the measured elevation of the sea level proxy*
SLP_CorrElev_m	*Elevation in meters of the sea level proxy corrected for the tide*
SLP_CorrElevErr_m	*Error in meters of the corrected elevation of the sea level proxy*
PSL_Elev_m	*Elevation in meters with respect to the present day mean sea level of the paleo sea level correlated with the geological remnant (data taken from Siddall et al., 2003)*
PSL_ElevErr_m	*Error in meters of the paleo sea level elevation (data taken from Siddall et al., 2003)*
OIS	*Oxygen isotope stage associated with the sea level proxy*
Age_ky	*Age of the sample in kiloyears*
Sample_code	*Code assigned to the sample in the field*
SampleElev_m	*Elevation of sample in meters*
SampleDepth_m	*Depth of sample below the local ground surface in meters*
Dating_method	*Method used for dating (AMS, U/Th, OSL, etc.)*
Lab_code	*Code assigned to the sample during the lab analyses*
Evidence	*Logical field taking values T = true and F = false. True is for records that can be used for calculating uplift rates*
LocalityName	*Local name of the site surveyed during field work*
Site_notes	*Description of the site*
Evidence_notes	*Comments on reliability and type of evidence for emergence*
SLP_notes	*Description of the sea level proxy (e.g.: notch, algal rim, lithophaga borings)*
PSL_notes	*References for the values and any other related information*
Age_notes	*Hints and warnings about the age of sample usually given by the lab that analyzed the sample*
Sample_notes	*Description of the sample*

Multitemporal InSAR Data and processing

A dataset of ERS and ENVISAT SAR images has been created selecting most of available SAR scenes covering the time span 1992-2009.

We have then applied the InSAR (Interferometric SAR) technique known as SBAS (Small Baseline Subset, IREA-CNR) dealing with the contemporary processing of a large dataset to provide surface velocity maps over the investigated area. The time series of displacement are also available for each point of the map. The result is the LOS (Line Of Sight) velocity that in this case is along 23° average incidence angle. SBAS technique allows the measurement of surface movements with an average accuracy of about 2 mm/y.

The processing method automatically discarded those scenes having too large spatial and/or temporal baselines with the others, extremely high doppler frequency shitfs and/or missing lines over a certain percentage. This constraints have reduced the total number of scenes really used to 44, 18 of which from ERS1-2 and 26 ENVISAT. This dataset covers the temporal interval from 1995 to 2009 (Figure 4).

The SBAS approach stems from the constraints for spatial and temporal baselines to generate a large number of image pairs respecting such thresholds. In this study we then obtained 85 interferograms (Figure 5).

Aiming at obtaining the widest possible spatial coverage we have generated more processing each referred to a specific reference point (stable for the hypothesis at the base of SBAS

procedure). Later on the velocity map provided is suitable to be verified and validated by means of external data, so as ground surveys.

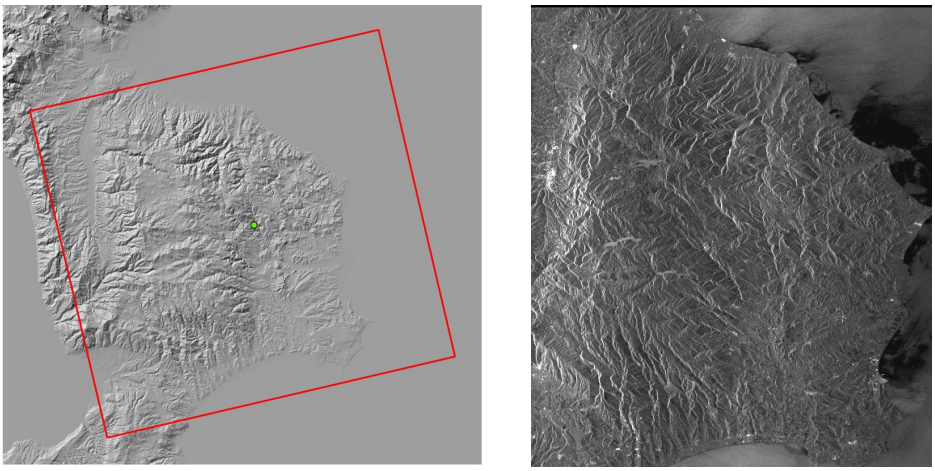

Figure 4 - The area covered by the selected SAR frame (red square in the left panel). Amplitude image of the focused master image (right panel).

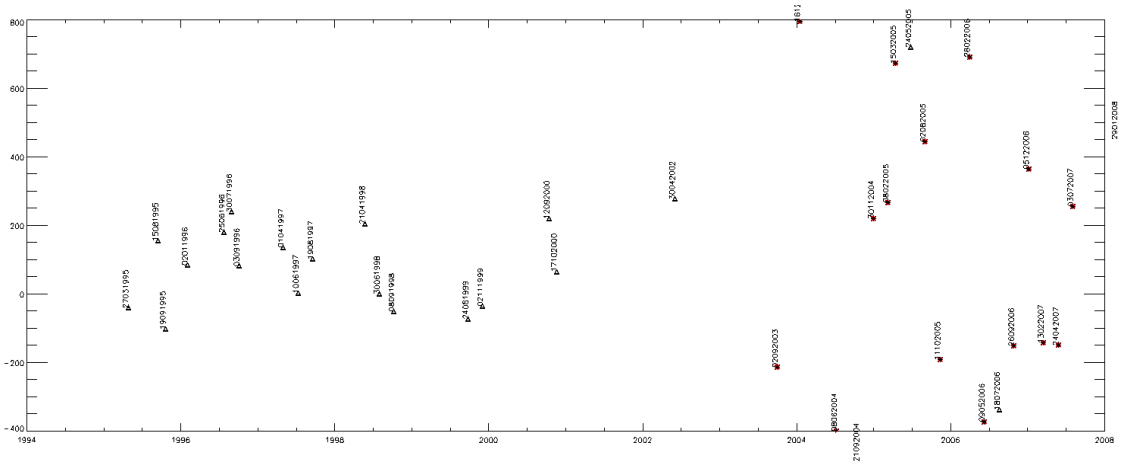

Figure 5 - Image distribution according to spatial and temporal baselines.

Three are the most reliable results, whose reference points are close to the coastline or nearby urban areas. Due to the very complex orography of the central portion of the study region (Sila plateau) and to the vegetation coverage in large portions of the study area the SBAS approach provided coherent points over limited areas and a wide propagation of the solution of the algorithm has been avoided. However, along the coastline where most of the areas of interest are concentrated the algorithm provided the best results in terms of density of coherent points.

Results

The three best results are shown in several maps (Figures 6-11). However, concerning the activities of the present project only the last one has been used for further studies in the framework of the UR. The reference "stable" point of this latter solution is close to the Crotone airport.

The results from the application of SBAS InSAR approach over the investigated region, covering the time interval 1995-2009, clearly highlight how the coast area ranging from

Catanzaro city up to the north area of Crotone city is characterized by a positive LOS velocity, meaning the surface is moving toward the sensor (uplift). This movement can be realistically justified as due to vertical displacements. The uplift of the coastline and the subsidence (red points) southward Crotone city seem justified from in situ surveys that described the presence of features in agreement with such vertical movements. In particular the area in subsidence is affected by well known landslides.

2. Relevance for DPC and/or for the scientific community

This study was largely experimental and unique in his kind. The investigated area is located in a region with the highest seismic hazard of Italy, affected by both crustal faults and a subduction zone. This type of study can shed light on the rate of deformation over different temporal scales and lead to better understand the relationships between long-term average deformation and local temporal transients.

3. Changes with respect to the original plans and reasons for it

Although we surveyed a much larger area, results illustrated here focus strictly on the Crotone Peninsula that is where we found more data on the different temporal scales, collectively.

4. References

Fleitmann D., Burns S.J., Mangini A., Mudelsee M., Kramers J., Villa I.M., Neff U., Al-Subbary A.A., Buettner A., Hippler D., Matter A. (2007). Holocene ITCZ and Indian monsoon dynamics recorded in stalagmites from Oman and Yemen (Socotra). Quaternary Science Reviews 26: 170–188.

Hippler D., Villa I.M., Nägler T.F., Kramers J.D. (2004). A ghost haunts mass spectrometry: real isotope fractionation or analytical paradox? Abstract, Goldschmidt Conference, København, A 215.

Ludwig K.R. (2003), User's Manual for Isoplot 3.00 a Geochronological Toolkit for Microsoft Excel, Berkeley Geochronology Center Special Publication vol. 4.

5. Key publications/presentations

None.

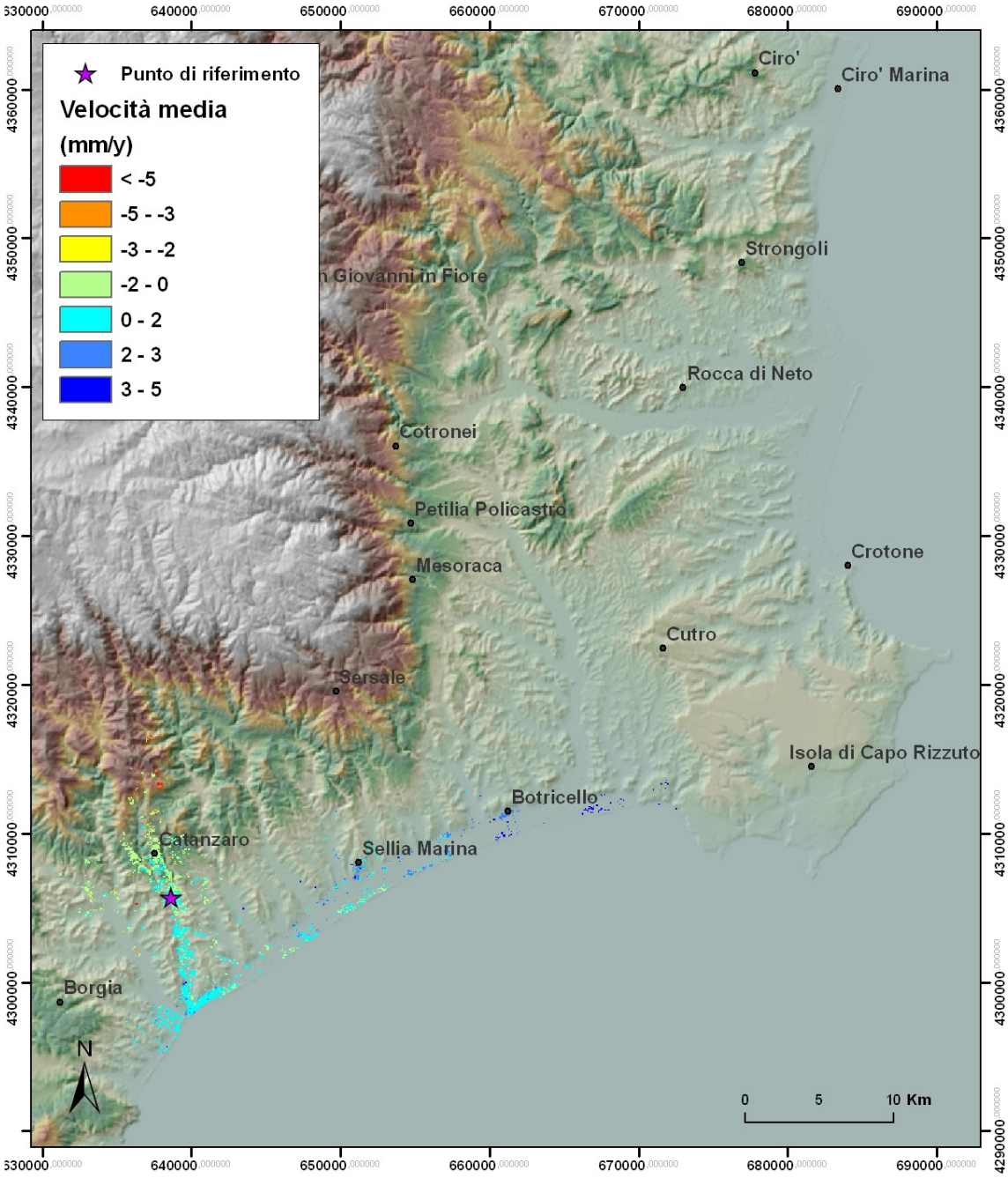

Figure 6 - LOS velocity map along ascending path. The reference point is nearby Catanzaro city.

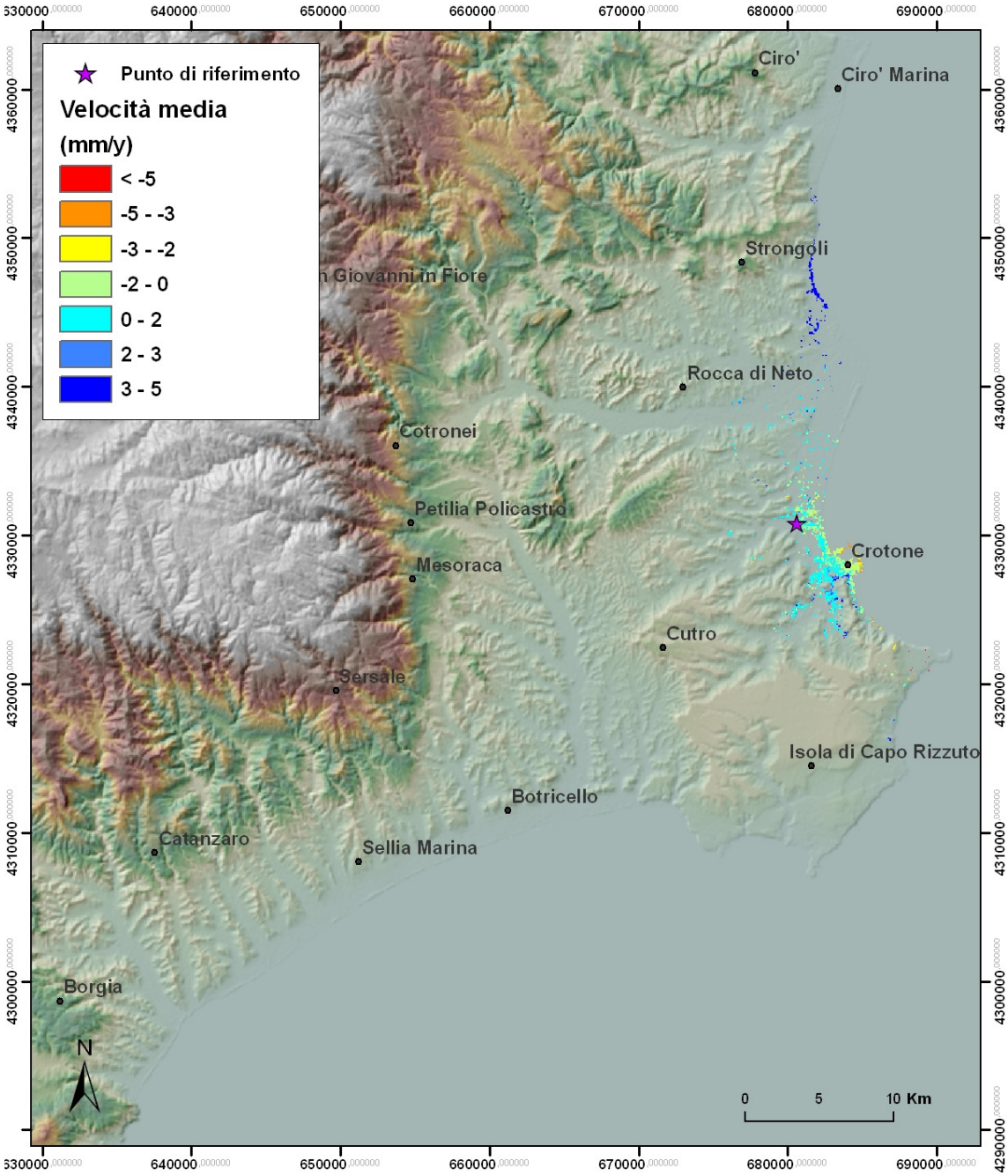

Figure 7 - LOS velocity map along ascending path. The reference point is nearby Crotone city.

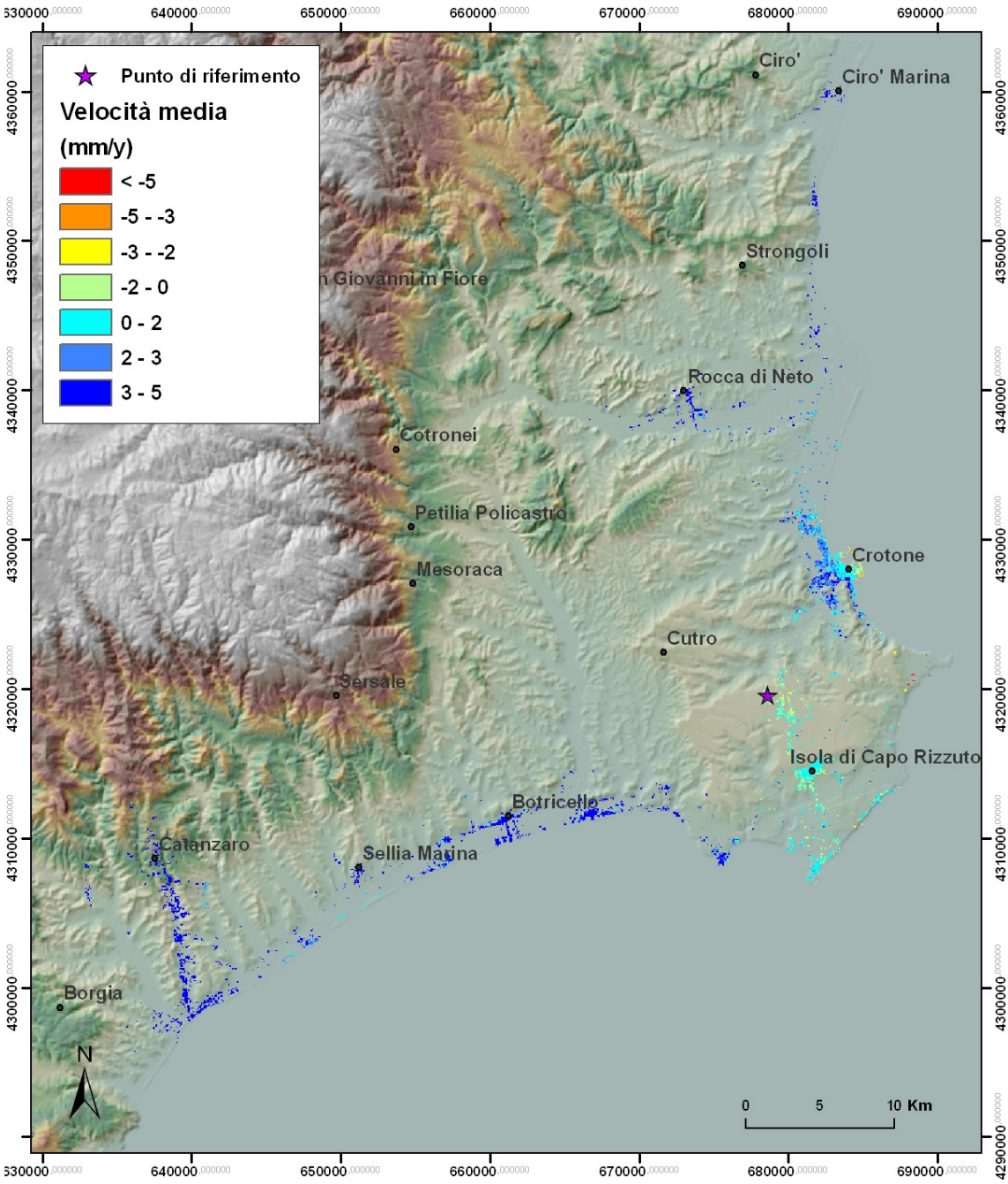

Figure 8 - LOS velocity map along ascending path. The reference point is nearby Isola di Capo Rizzuto village.

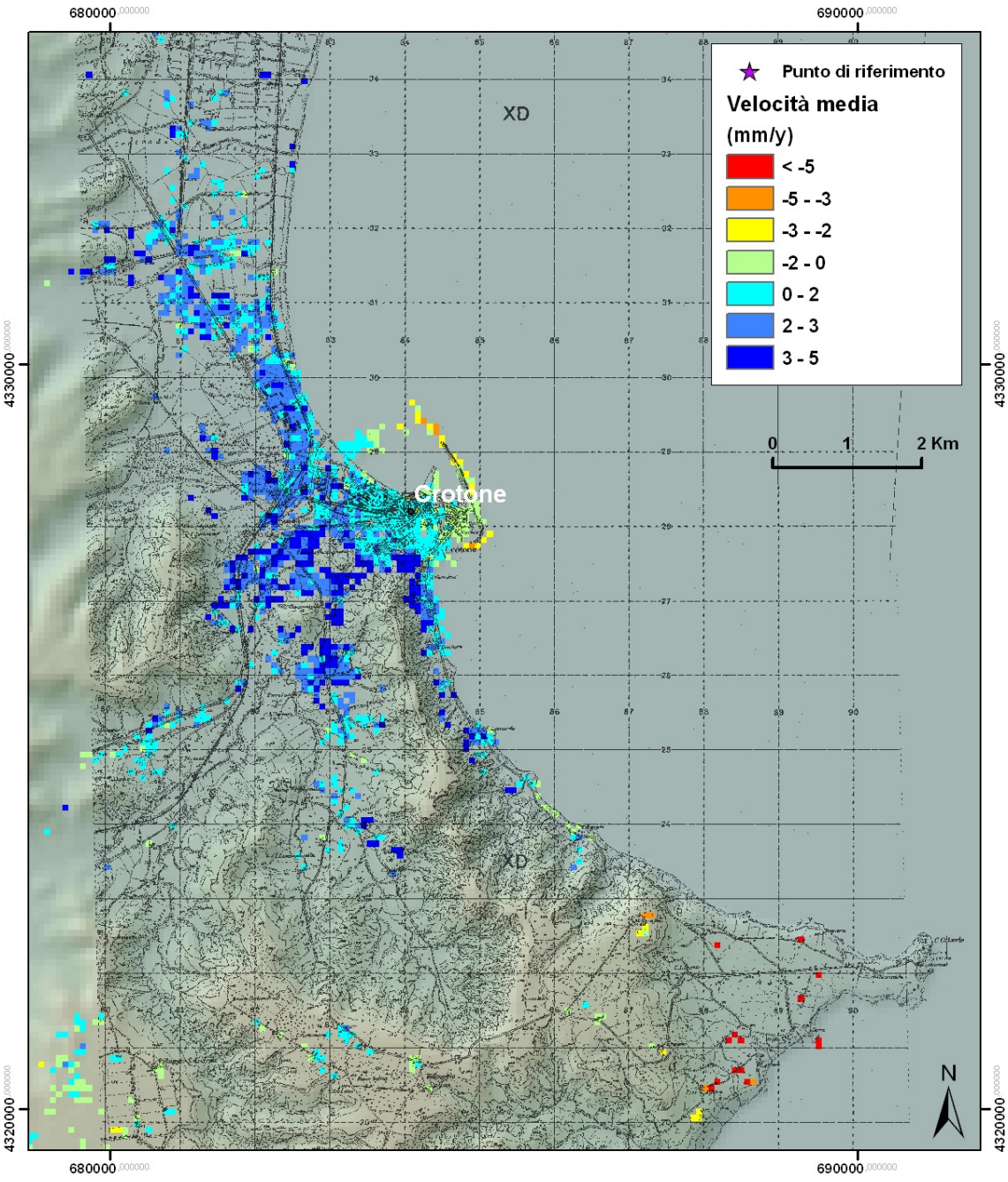

Figure 9 - Zoom in over Crotone from Figure 8.

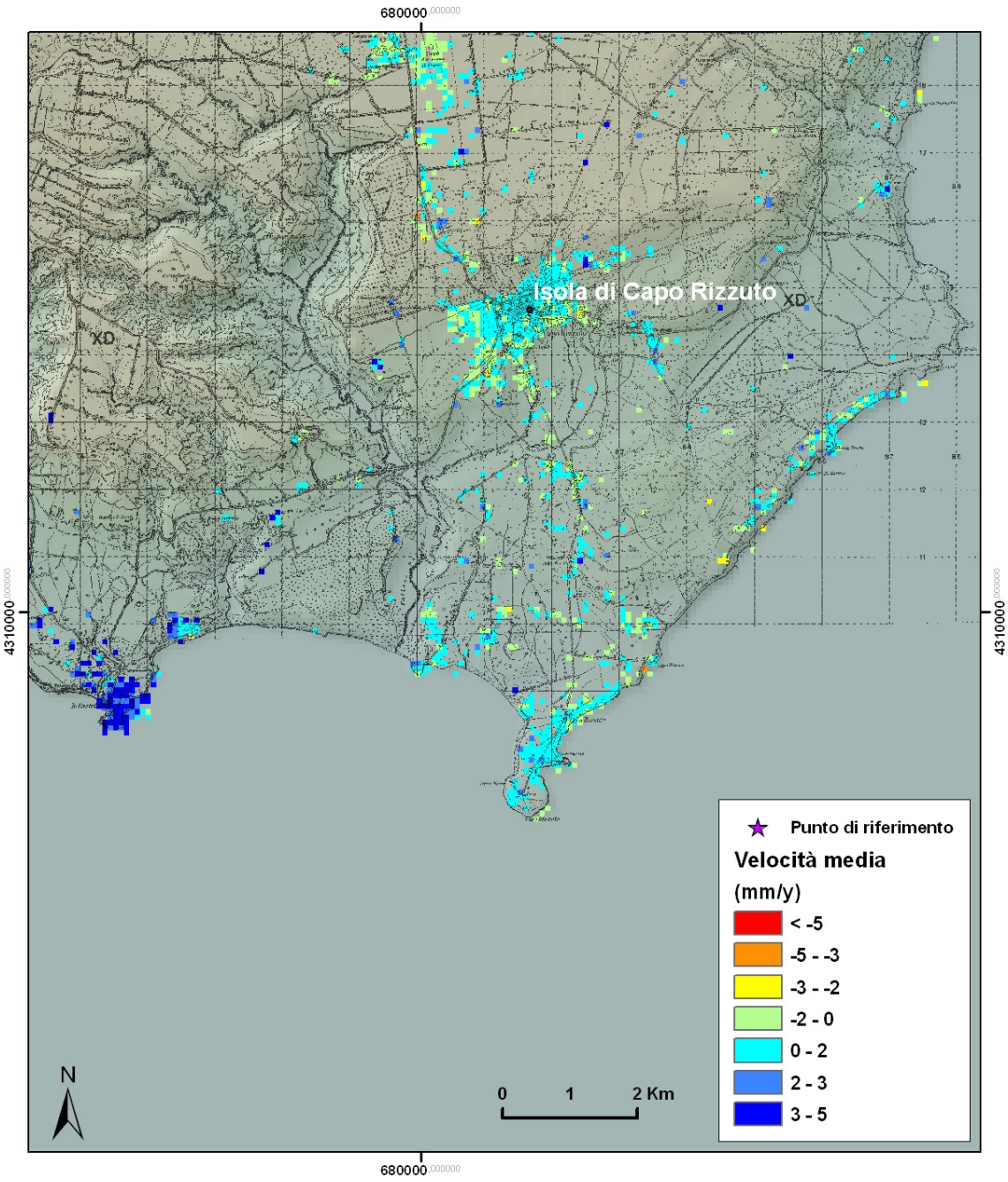

Figure 10 - Zoom in over Isola di Capo Rizzuto from Figure 8.

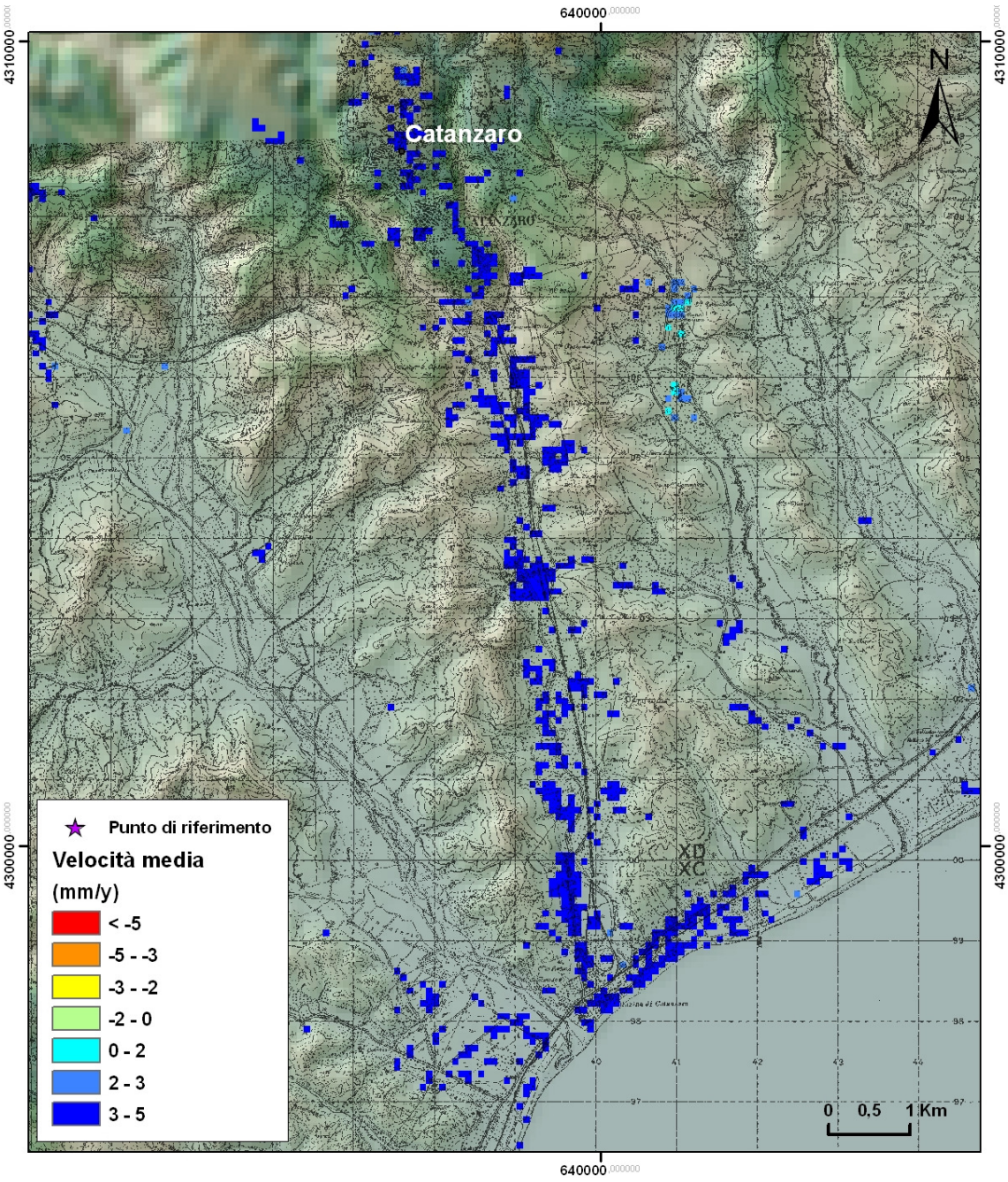

Figure 11 - Zoom in over Catanzaro city from Figure 8.

Table 1 – Summary of the terrace sites mapped during the field survey with description of the geomorphic markers.

ID	Locality	Lat	Lon	Site description	Sample type	Marker	Sample Available	Dating available	Age used
501	Capo Cimiti	38.957	17.171	About 5.80 m of bio-calcarenite and algal reef resting on the Cutro clays.	Coral found in a bio-calcarenite rock.	Terrace riser	T	T	F
502	Capo Colonna	39.023	17.204	About 4 m of bio-calcarenite and algal reefs resting on the Cutro clays.	Coral found in a bio-calcarenite rock.	Terrace riser	T	T	F
503	Marinella	38.986	17.163	Landslides: rotational slides, complex slides.	Coral found in a boulder fell from the lowermost terrace exposure.	Terrace riser	T	F	F
504	Le Castella	38.929	17	Deposit of about 7 m of thickness resting on the Cutro clays.	Loose coral sampled from the top of the deposit.	Terrace riser	T	T	T
505	Le Castella	38.928	17.017	Outer edge of the terrace.	Loose coral sampled from the top of the deposit.	Terrace riser	T	T	T
506	Le Castella	38.913	17.031	About 8 m of bio-calcarenites and algal reef resting on the Cutro clays.	Coral found in a bio-calcarenite rock.	Terrace riser	T	F	F
507	Capo Cimiti	38.952	17.165	About 5 m of bio-calcarenites and algal reef resting on the Cutro clays.	Coral found in a bio-calcarenite rock.	Terrace riser	T	T	T
508	Capo Colonna	39.028	17.192	About 3 m of bio-calcarenites.	Coral found in a bio-calcarenite rock.	Terrace riser	T	F	F
509	Capo Colonna	39.029	17.205	About 2 m of bio-calcarenites overlying a 10 m thick siliciclastic sandstones with storm and current structures.	Coral found in a bio-calcarenite rock.	Terrace riser	T	F	F
510	Le Castella	38.906	17.024	Abrasion platform on siliciclastic sandstones with storm and current structures.	Calcite filling a fracture in the terrace deposit after the terrace emergence. The wave-cut platform has to be older.	N/A	T	F	F
511	Isola di Capo Rizzut	38.949	17.074	Organic calcarenite with skeletal concentration, 1.5 m thick, resting on the Cutro clays.	Corals.	Terrace riser	T	F	F
512	Campolongo	38.97	17.016	Bio-calcarenites resting on the Cutro clays.	Corals.	Terrace riser	T	F	F
513	Campolongo	38.97	17.016	Bio-calcarenites resting on the Cutro clays.	Corals.	Terrace riser	T	F	F
514	Campolongo	38.936	17.014	Bio-calcarenites with skeletal concentration.	Corals.	Terrace riser	T	T	T
515	Rosito	38.999	17.003	Bio-calcarenites resting on the Cutro clays.	Corals.	Terrace	T	F	F
516	Isola di Capo Rizzut	38.95	17.083	Bio-calcarenites.	Corals.	Terrace riser	T	F	F
517	Isola di Capo Rizzut	38.942	17.073	Quarry, terrace tread; bio-calcarenites.	Corals.	Terrace tread	T	F	F
518	Capo Colonna	39.0296	17.1724	Capo Colonna terrace inner edge	None.	Inner edge	F	F	F
519	Capo Colonna	39.0249	17.1714	Capo Colonna terrace inner edge	None.	Inner edge	F	F	F
520	Capo Cimiti	38.9696	17.1465	Capo Cimiti terrace inner edge	None.	Inner edge	F	F	F
521	Capo Cimiti	38.9578	17.1311	Capo Cimiti terrace inner edge	None.	Inner edge	F	F	F
522	Le Castella	38.9346	17.0116	Le Castella terrace inner edge	None.	Inner edge	F	F	F
523	Le Castella	38.9306	17.0278	Le Castella terrace inner edge	None.	Inner edge	F	F	F
524	Campolongo	38.936	17.0182	Campolongo terrace inner edge	None.	Inner edge	F	F	F
525	Campolongo	38.933	17.0276	Campolongo terrace inner edge	None.	Inner edge	F	F	F
526	Isola di Capo Rizzut	38.9432	17.0772	Isola di Capo Rizzuto terrace inner edge	None.	Inner edge	F	F	F
527	Isola di Capo Rizzut	38.9559	17.068	Lower Cutro terrace inner edge	None.	Inner edge	F	F	F
528	Isola di Capo Rizzut	38.9578	17.0744	Lower Cutro terrace inner edge	None.	Inner edge	F	F	F

Table 2 – Summary of the coastline sites mapped during the field survey with description of the geomorphic markers.

ID	Locality	Lat	Lon	Site description	Marker	Sample available	Dating available	Evidence
101	Campolongo	38.930	16.997	Boulders on a sandy beach with lithophaga borings.	Lithopaga borings on boulders.	T	T	Evidence of emergence but not of Holocene Age.
102	Le Castella	38.906	17.024	Raised abrasion platforms on marine terrace deposits.	Raised abrasion platforms.	F	F	Evidence of emergence, possibly Holocene (no samples for datings available).
103-111; 132	Bosco Soverito	38.918	17.057	Raised beach with notch and sandy dunes at the rear.	Notch.	T	T	Evidence of Holocene emergence.
112-113	Capo Piccolo and Capo Rizzuto	38.912	17.075	Coast with vegetation and buildings, and steep clayey cliff topped by terrace.	N/A	F	F	No evidence of Holocene emergence.
114	Pizzo Greco	38.924	17.127	Boulders on a sandy beach with encrusting serpulides.	Encrusting serpulides on boulders.	T	F	Doubtful evidence of emergence.
115-125	Chiacolilli sud	38.930	17.134	Raised abrasion platforms and notches.	Raised abrasion platforms and notches.	F	F	Evidence of emergence, possibly Holocene (no samples for datings available).
126	Chiacolilli	38.932	17.137	Beachrock slabs with algal rim concretions.	Algal rim.	T	T	Evidence of Holocene emergence.
127	Curmo	38.938	17.143	Boulders on a sandy beach encrusted with doubtful algal rim.	Doubtful algal rim on boulders.	T	F	Doubtful evidence of emergence.
128	Marinella	38.986	17.163	Clayey cliff with a raised beach at the top.	Raised beach.	T	T	Evidence of emergence but not of Holocene Age.
129	Domine Maria	38.999	17.168	Boulders on a sandy beach at a river mouth with notch and lithophaga borings.	Notch, lithophaga borings and algal rim on boulders.	F	F	Doubtful evidence of emergence.
130-131	Capo Colonna	39.029	17.205	Algal encrustations of a boulder located at about - 8m from the top of the lower Capo Colonna terrace.	Algal rim.	T	T	Evidence of emergence but not of Holocene Age.
133	Capo Cimiti	38.957	17.171	Steep clayey cliff topped by terrace.	N/A	F	F	No evidence of Holocene emergence.

Table 3 - U/Th Dating Results

Sample name	232Th/238U	2SE	230Th/238U	2SE	234U/238U	2SE	230Th/232Th	2SE	ppb U	2SE	Single-point age (ka)	3D Isochron age (ka)
KR 254 A	0.0678	0.0003	1.230	0.028	1.120	0.001	18.13	0.42	897.15	1.25	Unreliable age because of open-system condition	
KR 254 B	0.0656	0.0003	1.198	0.012	1.113	0.001	18.26	0.20	945.69	1.29		
KR 257 A	0.0634	0.0003	0.849	0.004	1.134	0.001	13.39	0.08	3078.61	4.37	-	138 ± 25
KR 257 B	0.0970	0.0005	0.854	0.005	1.120	0.001	8.80	0.07	2499.81	3.46	-	
KR 257 C	0.0275	0.0001	0.849	0.004	1.131	0.001	30.88	0.19	3333.23	4.53	-	
KR 257 D	0.0343	0.0002	0.812	0.006	1.127	0.001	23.66	0.20	3474.17	4.75	133 ± 3	
KR 261 A	0.2526	0.0010	0.805	0.008	1.110	0.001	3.19	0.03	688.39	0.95	-	118 ± 54
KR 261 B	0.4268	0.0021	1.003	0.007	1.117	0.001	2.35	0.02	445.61	0.62	-	
KR 261 C	0.1132	0.0005	0.862	0.006	1.121	0.001	7.62	0.06	977.67	1.33	152 ± 4	
KR 261 D	0.2161	0.0010	0.802	0.006	1.114	0.001	3.71	0.03	537.35	0.74	-	
KR 268 A	0.1662	0.0009	0.884	0.005	1.118	0.001	5.32	0.04	639.77	1.06		
KR 268 B	0.1636	0.0006	1.171	0.014	1.124	0.001	7.16	0.09	362.16	0.50	Unreliable age because of open-system condition	
KR 268 C	0.2542	0.0014	0.904	0.006	1.139	0.001	3.56	0.03	536.69	0.72		
KR 268 D	0.2894	0.0015	1.319	0.009	1.132	0.002	4.56	0.04	315.74	0.45		
KR 258 A	0.0183	0.0001	0.821	0.005	1.119	0.001	44.84	0.35	3553.76	5.00	-	162 ± 68
KR 258 B	0.0158	0.0001	0.772	0.003	1.141	0.001	48.87	0.32	3699.49	5.20	119 ± 2	
KR 258 C	0.0091	0.0001	0.710	0.009	1.130	0.001	77.99	1.05	3534.57	4.99	-	
KR 258 D	0.0485	0.0004	0.515	0.005	1.132	0.001	10.62	0.13	3623.43	5.07	-	
KR 459 A	0.0163	0.0002	0.854	0.001	1.137	0.001	52.40	0.50	2902.392	4.32	145 ± 4	-
KR 355	0.0019	0.0005	0.073	0.002	1.084	0.002	37.53	0.29	393.1715	0.63	7.6 ± 0.2	-

Table 4 – Summary of radiocarbon dated samples.

Lab code	Locality ID	Locality	Lat	Lon	Marker elevation (m)	Error (±m)	Age (ky)	Error (±ky)	Cal Age BP 2sigma	Description
Poz-31064	130-131	Capo Colonna	39.029	17.205	6.74	0.25	29.120	0.26	-	Algal concretion with fragments of corals and bivalves.
Poz-31063	130-131	Capo Colonna	39.029	17.205	6.74	0.25	31.340	0.34	-	Bivalve shell of KR202A.
Poz-31067	101	Campolongo	38.930	16.997	1.92	0.50	42.300	1.20	-	Lithophaga shell in a boulder on a sandy beach.
Poz-31066	126	Chiacolilli	38.932	17.137	1.43	0.20	2.560	0.03	2140-2317	Algal rim on a beachrock slab.
Poz-31068	128	Marinella	38.986	17.163	3.81	0.50	35.100	0.50	-	Bivalve shell in a raised beach.
Beta - 261643	103-111; 132	Bosco Soverito	38.918	17.057	1.02	0.50	4.880	0.040	5300-5040	Lithophaga shell found in living position.
Beta - 261644	103-111; 132	Bosco Soverito	38.918	17.057	1.18	0.20	3.760	0.040	3810-3590	Algal rim, also with serpulides.
Beta-279336	103-111; 132	Bosco Soverito	38.918	17.059	0.84	0.20	0.00	0.050	-	Lithophaga shell found in living position. Possible 18th, 19th, or 20th century.